Neutron-proton isovector pairing correlations treatment in heated nuclei within the path integral formalism

M. Fellah N.H. Allal M.R. Oudih

Laboratoire de Physique Théorique- Faculté de Physique- USTHB, BP32 El-Alia, 16111 Bab-Ezzouar - ALGER - ALGERIA

Abstract: A method for the treatment of the neutron-proton (np) isovector pairing correlations at finite temperature is developed within the path integral formalism. It generalizes the recently proposed model using a similar approach in the pairing between like-particles case. The pairing terms in the total Hamiltonian are written in a square form in order to facilitate the use of the Hubbard-Stratonovitch transformation. The expression for the partition function of the system is then established. The gap equations, as well as the expressions for the energy, the entropy and the heat capacity of the system are deduced. As a first step, the formalism is numerically applied to the schematic Richardson model. As a second step, the method is applied to nuclei such as $N = Z$ using the single-particle energies of a deformed Woods-Saxon mean-field. The variations in the gap parameters, the excitation energy and the heat capacity are studied as functions of the temperature. It is shown that the overall behavior of these quantities is similar to their homologues in the standard FTBCS model. We note in particular the existence of critical temperatures beyond which the pairing vanish. Moreover, it appears that in the framework of the present approach, the pairing effects persist beyond the critical temperatures predicted by the FTBCS model in the pairing between like-particles case or its generalization in the np pairing case.

Keywords: Nuclear structure, Isovector pairing, Temperature, Path integral

DOI: 10.1088/1674-1137/adc4cb **CSTR:**

I. INTRODUCTION

Pairing correlations are of special importance in nuclear structure theory. They have an influence on many nuclear properties such as deformation, moments of inertia, etc... The pairing between like-particles (i.e. protons or neutrons) has been widely studied since the end of the 1950s when the Bardeen, Cooper and Schrieffer (BCS) theory of superconductivity [1] has been adapted to nuclear physics [2].

In $N \simeq Z$ nuclei, there is a large overlap between neutron and proton wave functions. It follows that besides the pairing between like-particles, there exists a neutron-proton (np) pairing. The latter may be of two different types namely the isovector pairing (T=1) and the isoscalar one (T=0). The first theoretical studies of np pairing by Goswami et al. [3]−[6] date from the 1960s. However, they were then somewhat abandoned for many years because the nuclei in which this type of pairing exists could not be observed experimentally. When the experimental study of these nuclei was made possible with the advent of radioactive ion beams, np pairing was the subject of a marked revival of interest over the last 25 years in both theoretical and experimental [7] sides. Many methods have been developed to describe both types of np pairing. A generalized BCS approach is often used (see e.g. [8]−[14], for a review see Refs [15]−[16]), because of its ease of use. It was applied in order to study various nuclear quantities such as the moment of inertia [17] or the one-proton and two-proton separation energies [18].

As the BCS method breaks the particle-number conservation symmetry, several studies have been devoted to the particle-number fluctuations in the np pairing case, as the Lipkin-Nogami method [19]−[23] which conserves approximately the particle-number. The restoration of the broken symmetry may also be performed using various approaches as particle-number projection methods either before (see e.g. [24]−[26]) or after the variation (see e.g. [27]−[31]). These methods have been applied to the study of various nuclear observables as the electric quadrupole moments [32], the beta transition probabilities [33] -[34], the charge, proton and neutron systems and matter radii [35], the moment of inertia [36] or the spectroscopic factors of various reactions [37]−[38].

Recently, a model based on the generator coordinate method has been developed in order to include the np pairing correlations. It was applied to the study of magnetic properties of $N = Z$ odd-odd nuclei [39].

Another possible approach consists of describing $N = Z$ systems where there exists a np pairing using α-

Received 3 March 2025; Accepted 25 March 2025

like quartets (see Ref. [40] and references therein).

On the other hand, np pairing effect may be analyzed by a shell model mean-field where the isovector pairing Hamiltonian can be built by using generators of the quasi-spin O(5) group [41]−[42]. A shell-model-like approach based on the relativistic density functional theory may also be used [43].

A completely different way to proceed consists of describing the np pairing correlations on quantum computers using a variational quantum eigensolver approach [44].

Nevertheless, all the previously cited methods describe systems at zero temperature. The oldest method for taking into account the pairing correlations in heated nuclei is the finite temperature BCS (FTBCS) approach which is also among the most used [45]−[49]. Some methods are based on this approach as the BCS-average [55] - [57] or the particle-number projection methods, either of PBCS or FBCS types [50]−[54]. Another approach is the Hartree-Fock-Bogoliubov (HFB) one [58]−[65], which may be also in its relativistic form [66]. In addition to the previously mentioned models, there are other methods like the random-phase-approximation [67]−[71], the covariant density functional theory [72]−[76], or the Matsubara formalism [77], as well as the self-consistent Green's function approach [78] or the generalized Lipkin-Nogami model [79]. For a review, see Ref. [80].

Another way to study the thermal pairing effect is the path integral technique in the framework of the shell-model Monte-Carlo method (SMMC) [81] -[83] or in a more convenient form in the static-path approximation [84]−[90]. Let us also cite the work of Fletcher [91] who has shown that the path integral formalism enables one to retrieve the FTBCS results using some approximations.

However, all these studies deal with the pairing between like-particles. Only few studies were devoted to the np pairing correlations at finite temperature. The most used methods are the shell model [92]−[95] and the SMMC [96]−[97]. More recently, the finite temperature np quasiparticle-random-phase-approximation was used in the study of Gamow-Teller excitations [98]. In Ref. [99], the phase diagrams for np superfluidity was investigated in asymmetric nuclear matter with inclusion of the angular dependence of the pairing gap.

In Refs [100]−[102], the np temperature dependent isovector pairing correlations are studied in the framework of the path integral technique using a generalization of the Fletcher method, whereas the isovector plus isoscalar ones are studied in Ref. [103].

Recently, we proposed a method for the treatment of pairing correlations between like-particles at finite temperature within the path integral formalism, based on the square-root extraction of the pairing term in the Hamiltonian of the system [104]. The aim of the present work is to generalize this method to the np pairing case. For simplicity, we consider only isovector pairing correlations.

The paper is organized as follows: Secs. II and III respectively deal with the Hamiltonian of the system and the derivation of the partition function. The gap equations and the expressions for the statistical quantities are established in Sec. IV. Numerical results are presented and discussed in Sec. V. Main conclusions are summarized in last section.

II. HAMILTONIAN

Let us consider a system of N neutrons and Z protons. In the isovector pairing case, it can be described, in the second quantization and isospin formalism, by the total Hamiltonian [3], [11], [15], [16]

$$\mathcal{H} = \sum_{\nu>0,t} \varepsilon_{\nu t}\left(a^{+}_{\nu t}a_{\nu t} + a^{+}_{\tilde{\nu}t}a_{\tilde{\nu}t}\right) - \sum_{t} G_{tt}P^{+}_{t}P_{t} - G_{np}P^{+}_{np}P_{np}. \tag{1}$$

In this expression, $\varepsilon_{\nu t}$ are the single-particle energies and $t = n, p$ is the isospin component.

$a^{+}_{\nu t}$ $(a_{\nu t})$ is the creation (annihilation) operator of a nucleon in the $|\nu t\rangle$ state. The state $|\tilde{\nu}t\rangle$ is the time-reversed state of $|\nu t\rangle$. $G_{tt'}$ $(t,t' = n,p)$ are the pairing-strength which are assumed to be constant. We also assume that $G_{np} = G_{pn}$.

The operators P^{+}_{t} and P^{+}_{np} are defined by

$$P^{+}_{t} = \sum_{\nu>0} a^{+}_{\nu t}a^{+}_{\tilde{\nu}t} \tag{2}$$

$$P^{+}_{np} = \sum_{\nu>0}\left(a^{+}_{\nu p}a^{+}_{\tilde{\nu}n} + a^{+}_{\nu n}a^{+}_{\tilde{\nu}p}\right). \tag{3}$$

Indeed, given the presence of the isospin quantum number t in the expression of $\mathcal{H}$, nucleons can interact with each other and create proton-proton, neutron-neutron and neutron-proton pairs while respecting the Pauli principle.

In order to conserve, on average, the particle numbers, we define the auxiliary Hamiltonian as

$$H = \mathcal{H} - \sum_{t}\lambda_{t}N_{t} \tag{4}$$

where λ_{t} is the Fermi level and N_{t} is the particle-number operator of a like-particles system (neutron or proton) defined by

$$N_{t} = \sum_{\nu>0}\left(a^{+}_{\nu t}a_{\nu t} + a^{+}_{\tilde{\nu}t}a_{\tilde{\nu}t}\right) \tag{5}$$

H may then be written

$$H = H_0 + H_1 \tag{6}$$

where we use the notations

$$H_0 = \sum_{\nu>0,t} \tilde{\varepsilon}_{\nu t}\left(\eta_{\nu t} + \eta_{\tilde{\nu} t}\right) \tag{7}$$

$$H_1 = \sum_t H_{tt} + H_{np} \tag{8}$$

$$H_{tt} = -G_{tt} P_t^+ P_t \ , \ H_{np} = -G_{np} P_{np}^+ P_{np} \tag{9}$$

$$\tilde{\varepsilon}_{\nu t} = \varepsilon_{\nu t} - \lambda_t \ , \tag{10}$$

$$\eta_{\nu t} = a_{\nu t}^+ a_{\nu t} \ . \tag{11}$$

It was shown in Ref. [104] that H_{tt} may take the form

$$H_{tt} = -G_{tt} R_{tt}^2 \tag{12}$$

with

$$R_{tt} = \sum_{\nu>0} \eta_{\nu t} \eta_{\tilde{\nu} t} B_{\nu t}, \tag{13}$$

where

$$B_{\nu t} = \prod_{\substack{j>0 \\ j\neq\nu}} \mathcal{S}_{jt} \ , \ \mathcal{S}_{jt} = i\left(a_{jt} + a_{j\tilde{t}}^+\right)\left(a_{\tilde{j}t} + a_{\tilde{j}\tilde{t}}^+\right). \tag{14}$$

As for the operator H_{np}, it may be written

$$H_{np} = -G_{np} R_{np}^2 \tag{15}$$

where

$$R_{np} = \sum_{\nu>0} \left[\eta_{\nu n}\eta_{\tilde{\nu} p} B_{\nu n\tilde{p}} + \eta_{\nu p}\eta_{\tilde{\nu} n} B_{\nu p\tilde{n}}\right] \tag{16}$$

with

$$B_{\nu n\tilde{p}} = \left(a_{\tilde{\nu} n} + a_{\tilde{\nu} n}^+\right)\left(a_{\nu p} + a_{\nu p}^+\right)\prod_{\substack{j>0 \\ j\neq\nu}} \mathcal{S}_{jn}\,\mathcal{S}_{jp} \tag{17}$$

$$B_{\nu p\tilde{n}} = \left(a_{\tilde{\nu} p} + a_{\tilde{\nu} p}^+\right)\left(a_{\nu n} + a_{\nu n}^+\right)\prod_{\substack{j>0 \\ j\neq\nu}} \mathcal{S}_{jn}\,\mathcal{S}_{jp}. \tag{18}$$

The calculation details are given in Appendix A.

III. GRAND PARTITION FUNCTION

The grand partition function is given by

$$Z = \mathrm{Tr} e^{-\beta H}, \tag{19}$$

where β is the inverse of the temperature T of the system and Tr is the trace over all the states of the system. Z is also given by

$$Z = \mathrm{Tr} e^{-\beta H_0} \mathsf{S}(\beta) \tag{20}$$

where the operator $\mathsf{S}(\beta)$ is defined by

$$\mathsf{S}(\beta) = e^{\beta H_0} e^{-\beta H}. \tag{21}$$

It may be written formally [104]

$$\mathsf{S}(\beta) = T_\tau \exp\left(\int_0^\beta H_1(\tau)\, d\tau\right) \tag{22}$$

T_τ being the chronological operator.

Using the definition (8) of H_1, $\mathsf{S}(\beta)$ becomes

$$\mathsf{S}(\beta) = T_\tau \ \exp\left(\int_0^\beta H_{nn}(\tau)\, d\tau\right) \times \exp\left(\int_0^\beta H_{pp}(\tau)\, d\tau\right) \exp\left(\int_0^\beta H_{np}(\tau)\, d\tau\right) \tag{23}$$

where we assumed that H_{nn} and H_{pp} commute with H_{np}. Indeed, the commutators $\left[H_{tt}, H_{np}\right]$, are proportional to the products $G_{tt}G_{np}$, which are small compared to the single-particle energies.

It is shown in Appendix B that Z takes the form

$$Z = \frac{1}{\pi^{3/2}\sqrt{G_{nn}G_{pp}G_{np}}} \int d\Delta_{nn} d\Delta_{pp} d\Delta_{np} \exp \times \left\{-\beta\left[\frac{|\Delta_{nn}|^2}{G_{nn}} + \frac{|\Delta_{pp}|^2}{G_{pp}} + \frac{|\Delta_{np}|^2}{G_{np}}\right]\right\} Tr \exp \times \left(-\beta \sum_\nu h_{\nu np}\right) \tag{24}$$

with

$$h_{\nu np}=\tilde{\varepsilon}_{\nu n}\left(\eta_{\nu n}+\eta_{\tilde{\nu}n}\right)+\tilde{\varepsilon}_{\nu p}\left(\eta_{\nu p}+\eta_{\tilde{\nu}p}\right)+2\Delta_{nn}\eta_{\nu n}\eta_{\tilde{\nu}n}B_{\nu n}+2\Delta_{pp}\eta_{\nu p}\eta_{\tilde{\nu}p}B_{\nu p}+2\Delta_{np}\left(\eta_{\nu n}\eta_{\tilde{\nu}p}B_{\nu n\tilde{p}}+\eta_{\tilde{\nu}n}\eta_{\nu p}B_{\nu p\tilde{n}}\right) \tag{25}$$

In the following, we will admit that the $h_{\nu np}$ and $h_{\mu np}$ operators commute when $\nu\neq\mu$. (see Appendix C for the justification)

We then have

$$\mathrm{Tr}\exp\left(-\beta\sum_{\nu}h_{\nu np}\right)=\prod_{\nu}\mathrm{Tr}\exp\left(-\beta h_{\nu np}\right). \tag{26}$$

All the operators in the expression for $h_{\nu np}$ commute with each other and act on different spaces. The eigenvalues of operators $\eta_{\nu t}$ are 0 and 1, those of $\eta_{\tilde{\nu}t}$ are the same. Dealing with operators $B_{\nu t}$, $B_{\nu n\tilde{p}}$ and $B_{\nu\tilde{n}p}$, each of them has the eigenvalues -1 and 1. Then, after some algebra, the partition function takes the form

$$Z=\frac{1}{\pi^{3/2}\sqrt{G_{nn}G_{pp}G_{np}}}\int d\Delta_{nn}d\Delta_{pp}d\Delta_{np}\exp\left\{-\beta\left[\frac{|\Delta_{nn}|^2}{G_{nn}}+\frac{|\Delta_{pp}|^2}{G_{pp}}+\frac{|\Delta_{np}|^2}{G_{np}}\right]\right\}\times\prod_{\nu}(8A_{\nu}) \tag{27}$$

where A_{ν} is defined by

$$A_{\nu}=2\left(1+2e^{-\beta\tilde{\varepsilon}_{\nu n}}+e^{-2\beta\tilde{\varepsilon}_{\nu n}}\cosh 2\beta\Delta_{nn}\right)\times\left(1+2e^{-\beta\tilde{\varepsilon}_{\nu p}}+e^{-2\beta\tilde{\varepsilon}_{\nu p}}\cosh 2\beta\Delta_{pp}\right)+4\left(\cosh 2\beta\Delta_{np}-1\right)\left[e^{-\beta\left(\tilde{\varepsilon}_{\nu n}+\tilde{\varepsilon}_{\nu p}\right)}+e^{-\beta\left(2\tilde{\varepsilon}_{\nu n}+\tilde{\varepsilon}_{\nu p}\right)}\times\cosh 2\beta\Delta_{nn}+e^{-\beta\left(\tilde{\varepsilon}_{\nu n}+2\tilde{\varepsilon}_{\nu p}\right)}\cosh 2\beta\Delta_{pp}\right]+\left(\cosh 4\beta\Delta_{np}-1\right)e^{-2\beta\left(\tilde{\varepsilon}_{\nu n}+\tilde{\varepsilon}_{\nu p}\right)}\cosh 2\beta\Delta_{nn}\cosh 2\beta\Delta_{pp} \tag{28}$$

IV. GAP EQUATIONS- STATISTICAL QUANTITIES

The grand partition function enables one to find the free energy which is obtained using the relation

$$Z=\frac{1}{\pi^{3/2}\sqrt{G_{nn}G_{pp}G_{np}}}\int d\Delta_{nn}d\Delta_{pp}d\Delta_{np}e^{-\beta F}. \tag{29}$$

Using the previous expression for the partition function, we have

$$F=\frac{|\Delta_{nn}|^2}{G_{nn}}+\frac{|\Delta_{pp}|^2}{G_{pp}}+\frac{|\Delta_{np}|^2}{G_{np}}-\frac{1}{\beta}\sum_{\nu>0}\ln 8A_{\nu}. \tag{30}$$

The quantities $\Delta_{tt'}$ are interpreted as the gap parameters. Hereafter, they are assumed to be real.

In the saddle-point approximation, the dominant contribution to the partition function is found by determining the minimum value of the exponent in Eq. (29), i.e., [108]

$$\frac{\partial F}{\partial\Delta_{tt'}}=0. \tag{31}$$

Using this approximation, we obtain

$$\frac{\Delta_{nn}}{G_{nn}\sinh 2\beta\Delta_{nn}}=\sum_{\nu}\frac{1}{A_{\nu}}\left\{2e^{-2\beta\tilde{\varepsilon}_{\nu n}}\left(1+2e^{-\beta\tilde{\varepsilon}_{\nu p}}+e^{-2\beta\tilde{\varepsilon}_{\nu p}}\cosh 2\beta\Delta_{pp}\right)+4\left(\cosh 2\beta\Delta_{np}-1\right)e^{-\beta\left(2\tilde{\varepsilon}_{\nu n}+\tilde{\varepsilon}_{\nu p}\right)}+\left(\cosh 4\beta\Delta_{np}-1\right)e^{-2\beta\left(\tilde{\varepsilon}_{\nu n}+\tilde{\varepsilon}_{\nu p}\right)}\cosh 2\beta\Delta_{pp}\right\} \tag{32}$$

$$\frac{\Delta_{pp}}{G_{pp}\sinh 2\beta\Delta_{pp}}=\sum_{\nu}\frac{1}{A_{\nu}}\left\{2e^{-2\beta\tilde{\varepsilon}_{\nu p}}\left(1+2e^{-\beta\tilde{\varepsilon}_{\nu n}}+e^{-2\beta\tilde{\varepsilon}_{\nu n}}\cosh 2\beta\Delta_{nn}\right)+4\left(\cosh 2\beta\Delta_{np}-1\right)e^{-\beta\left(2\tilde{\varepsilon}_{\nu p}+\tilde{\varepsilon}_{\nu n}\right)}+\left(\cosh 4\beta\Delta_{np}-1\right)e^{-2\beta\left(\tilde{\varepsilon}_{\nu n}+\tilde{\varepsilon}_{\nu p}\right)}\cosh 2\beta\Delta_{nn}\right\} \tag{33}$$

$$\frac{\Delta_{np}}{4G_{np}\sinh 2\beta\Delta_{np}}=\sum_{\nu}\frac{1}{A_{\nu}}\left\{e^{-\beta\left(\tilde{\varepsilon}_{\nu n}+\tilde{\varepsilon}_{\nu p}\right)}+e^{-\beta\left(2\tilde{\varepsilon}_{\nu n}+\tilde{\varepsilon}_{\nu p}\right)}\cosh 2\beta\Delta_{nn}+e^{-\beta\left(2\tilde{\varepsilon}_{\nu p}+\tilde{\varepsilon}_{\nu n}\right)}\times\cosh 2\beta\Delta_{pp}+e^{-2\beta\left(\tilde{\varepsilon}_{\nu n}+\tilde{\varepsilon}_{\nu p}\right)}\times\cosh 2\beta\Delta_{nn}\cosh 2\beta\Delta_{pp}\cosh 2\beta\Delta_{np}\right\}. \tag{34}$$

The grand potential Ω is given by

$$\Omega=-\beta F. \tag{35}$$

The latter enables one to find the particle-numbers that are are defined by

$$N_t=\left.\frac{\partial\Omega}{\partial\alpha_t}\right|_{\beta=const.},\ \alpha_t=\beta\lambda_t\ . \tag{36}$$

After some algebra, they are given by

$$N_t = 2\sum_{\nu} N_{\nu t} \tag{37}$$

where we set

$$\begin{aligned} N_{\nu n} = \frac{1}{A_\nu}\Big\{ & 2e^{-\beta\tilde{\varepsilon}_{\nu n}}\left(1+e^{-\beta\tilde{\varepsilon}_{\nu n}}\cosh 2\beta\Delta_{nn}\right) \\ & \times\left(1+2e^{-\beta\tilde{\varepsilon}_{\nu p}}+e^{-2\beta\tilde{\varepsilon}_{\nu p}}\cosh 2\beta\Delta_{pp}\right) \\ & +2\left(\cosh 2\beta\Delta_{np}-1\right)e^{-\beta\left(\tilde{\varepsilon}_{\nu n}+\tilde{\varepsilon}_{\nu p}\right)} \\ & \times\left(1+2e^{-\beta\tilde{\varepsilon}_{\nu n}}\cosh 2\beta\Delta_{nn}+e^{-\beta\tilde{\varepsilon}_{\nu p}}\cosh 2\beta\Delta_{pp}\right) \\ & +\left(\cosh 4\beta\Delta_{np}-1\right)e^{-2\beta\left(\tilde{\varepsilon}_{\nu n}+\tilde{\varepsilon}_{\nu p}\right)} \\ & \times\cosh 2\beta\Delta_{nn}\cosh 2\beta\Delta_{pp}\Big\} \end{aligned} \tag{38}$$

$$\begin{aligned} N_{\nu p} = \frac{1}{A_\nu}\Big\{ & 2e^{-\beta\tilde{\varepsilon}_{\nu p}}\left(1+e^{-\beta\tilde{\varepsilon}_{\nu p}}\cosh 2\beta\Delta_{pp}\right) \\ & \times\left(1+2e^{-\beta\tilde{\varepsilon}_{\nu n}}+e^{-2\beta\tilde{\varepsilon}_{\nu n}}\cosh 2\beta\Delta_{nn}\right) \\ & +2\left(\cosh 2\beta\Delta_{np}-1\right)e^{-\beta\left(\tilde{\varepsilon}_{\nu n}+\tilde{\varepsilon}_{\nu p}\right)} \\ & \times\left(1+e^{-\beta\tilde{\varepsilon}_{\nu n}}\cosh 2\beta\Delta_{nn}+2e^{-\beta\tilde{\varepsilon}_{\nu p}}\cosh 2\beta\Delta_{pp}\right) \\ & +\left(\cosh 4\beta\Delta_{np}-1\right)e^{-2\beta\left(\tilde{\varepsilon}_{\nu n}+\tilde{\varepsilon}_{\nu p}\right)} \\ & \times\cosh 2\beta\Delta_{nn}\cosh 2\beta\Delta_{pp}\Big\}. \end{aligned} \tag{39}$$

The system formed by the definitions of the gap parameters (Eqs. (32)-(34)) and the particle-number conservation conditions (Eqs. (38)-(39)) constitutes the gap equations.

At the limit where $\Delta_{np}=0$, these equations become

$$\begin{aligned} \frac{\Delta_{tt}}{G_{tt}} = & \sinh(2\beta\Delta_{tt}) \\ & \times\sum_{\nu}\frac{e^{-2\beta\tilde{\varepsilon}_{\nu t}}}{1+2e^{-\beta\tilde{\varepsilon}_{\nu t}}+e^{-2\beta\tilde{\varepsilon}_{\nu t}}.\cosh(2\beta\Delta_{tt})} \end{aligned} \tag{40}$$

$$N_t = 2\sum_{\nu}\frac{e^{-\beta\tilde{\varepsilon}_{\nu t}}+e^{-2\beta\tilde{\varepsilon}_{\nu t}}.\cosh(2\beta\Delta_{tt})}{1+2e^{-\beta\tilde{\varepsilon}_{\nu t}}+e^{-2\beta\tilde{\varepsilon}_{\nu t}}.\cosh(2\beta\Delta_{tt})}. \tag{41}$$

They correspond to the gap equations in the pairing between like-particles case of Ref. [104].

Moreover, the gap equations of the present study are different from those of Refs. [100−102] in the isovector pairing case which are recalled in Appendix D. Indeed, even if both methods are based on the path integral approach, the approximations introduced in order to use the Hubbard-Stratonovitch transformation are different.

The energy of the system may also be derived using the grand potential Ω. It is defined by

$$E = -\left.\frac{\partial\Omega}{\partial\beta}\right|_{\alpha_t=const},\ \alpha_t=\beta\lambda_t. \tag{42}$$

After some algebra, it is given by

$$E = -\frac{\Delta_{nn}^2}{G_{nn}}-\frac{\Delta_{pp}^2}{G_{pp}}-\frac{\Delta_{np}^2}{G_{np}}+2\sum_{\nu,t}\varepsilon_{\nu t}N_{\nu t}. \tag{43}$$

The entropy is defined by

$$S = \Omega-\beta\sum_t\lambda_t N_t+\beta E, \tag{44}$$

and the heat capacity by

$$C = T\frac{\partial S}{\partial T} = -\beta\frac{\partial S}{\partial\beta} \tag{45}$$

V. NUMERICAL RESULTS AND DISCUSSION

The previously described formalism has been first tested using the schematic Richardson model and then applied to realistic cases.

A. Richardson model

In the Richardson model [109], the single-particle levels are doubly degenerated and equidistant. They are such that

$$\varepsilon_{\nu t} = \nu\ ,\ \nu = 1,2,..,Nor,\ t = n,p, \tag{46}$$

where Nor is the total degeneracy of the levels.

We consider the system $N=Z=10$, $Nor=10$, since the np pairing exists essentially in nuclei such $N\simeq Z$. The pairing-strength constants $G_{tt'}$ have been chosen such as to reproduce the values of the gap parameters $\Delta_{tt'}$ at zero temperature. We chose arbitrarily the following values

$$\Delta_{nn}(0) = 1.4MeV$$
$$\Delta_{pp}(0) = 1.2MeV$$
$$\Delta_{np}(0) = 0.3MeV.$$

The values of $\Delta_{nn}(0)$ and $\Delta_{pp}(0)$ are intentionally chosen different so that the curves $\Delta_{nn}(T)$ and $\Delta_{pp}(T)$ are not superposed. The $\Delta_{np}(0)$ value is significantly lower than $\Delta_{nn}(0)$ and $\Delta_{pp}(0)$ in order to reproduce the realistic

cases (see below).

1. *Gap parameters*

The variations in the various gap parameters as functions of the temperature are shown in Fig. 1. They are compared to the results obtained using the method described in Refs [100−102] in the isovector np pairing case. In what follows, the present method will be designated by the abbreviation NP-1 and that of Refs [100−102] by the abbreviation NP-2. The variations of $\Delta_{tt}(T)$ in the pairing between like-particles case obtained using the method described in Ref. [104] (designated by the abbreviation LP-1) and the standard FTBCS method (designated by the abbreviation LP-2) are also reported in the same figure.

Surprisingly, the $\Delta_{tt}(T)$ curves of the present work overlap with those of method LP-1. We see from the figure that the behavior of $\Delta_{tt'}(T)$ of the present work is similar to that of $\Delta_{nn}(T)$ and $\Delta_{pp}(T)$ in the standard FTBCS method (LP-2). We note in particular the existence of critical temperatures (which will be noted $T_{ctt'}$, $t,t'=n,p$, in what follows) beyond which the gap parameters vanish. However, their values are significantly higher than the values obtained in both LP-2 and NP-2 methods. The present model therefore predicts the existence of an isovector pairing at temperatures beyond what the NP-2 model predicts. Unfortunately, there are no exact values in the isovector pairing case, as in the like-particle case [110]. We cannot therefore decide between the two methods. However, NP-1 method is a generalization of LP-1, while NP-2 is a generalization of LP-2 (FTBCS). LP-1 reproduces exact values better than LP-2 in a wider temperature range (see Ref. [104]). This may suggest that the NP-1 results would be better than those of NP-2.

Besides, in the present method, the curves of $\Delta_{nn}(T)$ and $\Delta_{pp}(T)$ show a plateau in the neighborhood of T_{cnp} whereas in method NP-2, they increase in the vicinity of T_{cnp} before decreasing from this value of T (see the enlarged part of Fig. 1). The fact that the NP-1 and NP-2 results are very different although the models are both developed within the path integral formalism is due to the nature of the approximations used. The latter are different in the two models.

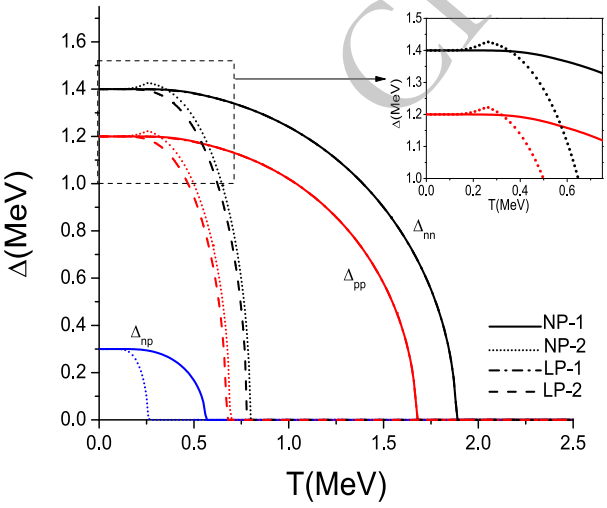

Fig. 1. (color online) Variation in the pairing gap parameter Δ_{nn} (in black),Δ_{pp} (in red), Δ_{np} (in blue) as functions of the temperature T within the framework of the Richardson model. Solid lines refer to the NP-1 model (present work), dotted lines refer to the NP-2 model (Refs [100−102]) in the isovector pairing case. Dash-dotted lines refer to the LP-1 model (Ref. [104]) and dashed lines refer to the LP-2 (standard FTBCS) model in the pairing between like-particles case. The Δ_{nn} and Δ_{pp} curves in NP-1 and LP-1 models are exactly superposed.

2. *Excitation energy*

In order to allow a comparison between the results of the various models, we consider the excitation energy E_{exc} defined as

$$E_{exc}(T)=E(T)-E(0), \tag{47}$$

rather than the energy of the system. The variations in $E_{exc}(T)$ are shown in Fig. 2 for the previously cited four models. The angular points which appear in each of these models correspond to the critical temperatures (see Fig.

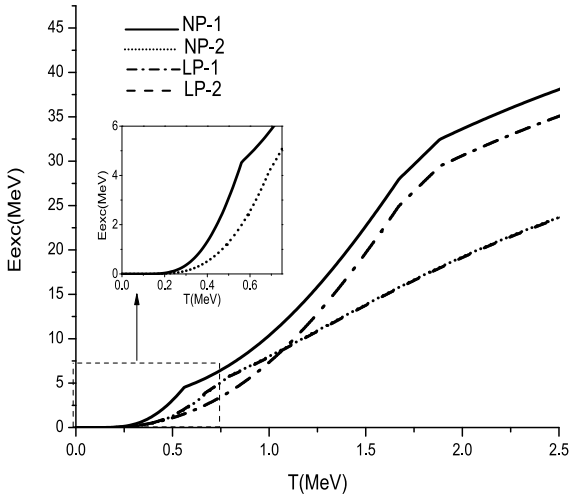

Fig. 2. Variation in the excitation energy $E_{exc}(T)$ as functions of the temperature T within the framework of the Richardson model. Solid lines refer to the NP-1 model (present work), dotted lines refer to the NP-2 model (Refs [100−102]) in the isovector pairing case. Dash-dotted lines refer to the LP-1 model (Ref. [104]) and dashed lines refer to the LP-2 (standard FTBCS) model in the pairing between like-particles case.

1). There are obviously three in the isovector pairing case and two in the like-particles pairing case.

In the isovector pairing case, it may be seen from the figure that, when $T < (T_{cnp})_1$, the increasing of E_{exc} is faster in model NP-1 than in model NP-2 (see the enlarged part of Fig. 2). Moreover, we can evaluate the isovector pairing effect using the discrepancies

$$\delta E_{exc1} = E_{exc}(NP\text{-}1) - E_{exc}(LP\text{-}1) \tag{48}$$

and

$$\delta E_{exc2} = E_{exc}(NP\text{-}2) - E_{exc}(LP\text{-}2), \tag{49}$$

since NP-1 (respectively NP-2) model is a generalization of LP-1 (respectively LP-2) model.

δE_{exc1} is clearly more important than δE_{exc2} which is very small. Indeed, the LP-2 and NP-2 graphs are very close to each other and appears superposed in the figure. This is due to the fact that the $\Delta_{pp}(T)$ and $\Delta_{nn}(T)$ graphs are very close in these two approaches (see Fig. 1). On the other hand, δE_{exc1} may reach up to 3 MeV. According to the present model, the isovector pairing effect on the excitation energy is therefore more important than what the NP-2 model predicts.

Beyond T_{cnn} of the present model, all curves are parallel since there is no more pairing in this region. However, in this temperature range, the graphs of $E_{exc}(T)$ are not superposed because the $E(0)$ values of are different in the various approaches.

3. *Heat capacity*

We have then studied the variation in the total heat capacity of the system C as functions of the temperature. The corresponding results are reported in Fig. 3 and compared to those obtained within NP-1, LP-1 and LP-2 methods.

From the figure, we see that the overall behavior is similar for the four approaches: the peaks correspond to the various critical temperatures. Indeed, the behavior of the pairing parameters is reflected in the heat capacity. In then appears that the present method does not enable one to reproduce the S-shaped curve of the experimental heat capacities [111−113]. This is due to the approximations used, namely on the one hand, the fact of assuming that the different terms of the total Hamiltonian commute, and on the other hand, to static-path and saddle-point approximations.

As was the case for the excitation energy, the curves of heat capacity obtained by methods NP-2 and LP-2 are practically superposed, even if there is a slight shift. Moreover, the peak corresponding to $(T_{cnp})_2$ is barely visible (see the enlarged part of Fig. 3).

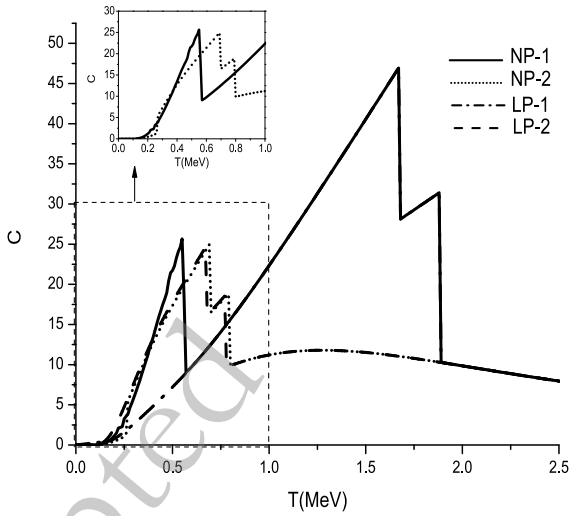

Fig. 3. Variation in the heat capacity C as functions of the temperature T within the framework of the Richardson model. Solid lines refer to the NP-1 model (present work), dotted lines refer to the NP-2 model (Refs [100−102]) in the isovector pairing case. Dash-dotted lines refer to the LP-1 model (Ref. [104]) and dashed lines refer to the LP-2 (standard FTBCS) model in the pairing between like-particles case.

We notice that the C values of the present study are significantly higher than those predicted by the other methods. The values at $T = T_{ctt'}$ are almost twice as large as in method NP-2.

Here again, the curves join beyond T_{cnn} of the present method, since there is no more pairing in this region.

B. Realistic cases

In realistic cases, we used the single-particle energies of a Woods-Saxon deformed mean-field with the parameters described in Ref. [114], with a maximum number of shells $N_{max} = 12$.

We consider in what follows three nuclei chosen as illustrative examples: ^{36}Ar, ^{48}Cr and ^{64}Ge. These nuclei are such as $N = Z$, since the np pairing is supposed to be maximal in this kind of systems. Moreover, for these nuclei, the pairing gap parameters $\Delta_{tt'}(0)$, $t,t' = n,p$, may be deduced from the even-odd mass differences. They are given by [12]:

$$\Delta_{pp} = -\frac{1}{8}[M(Z+2,N) - 4M(Z+1,N) + 6M(Z,N) - 4M(Z-1,N) - 4M(Z-2,N)] \tag{50}$$

$$\Delta_{nn} = -\frac{1}{8}[M(Z,N+2) - 4M(Z,N+1) + 6M(Z,N) - 4M(Z,N-1) - 4M(Z,N-2)] \tag{51}$$

$$\Delta_{np} = \frac{1}{4}\{2[M(Z,N+1)+M(Z,N-1) +M(Z-1,N)+M(Z+1,N)]-4M(Z,N) -[M(Z+1,N+1)+M(Z-1,N+1) +M(Z+1,N-1)+M(Z+1,N-1)]\} \quad (52)$$

where $M(Z,N)$ is the experimental mass value.

Besides, results concerning these nuclei obtained within the framework of the NP-2 method are available in Ref. [101]. Unfortunately, the nuclei for which semiexperimental heat capacity data is available like the ^{162}Dy and the ^{172}Yb which were considered in Ref. [104] have a large $(N-Z)$ value. In these nuclei, np pairing is negligible.

1. *Gap parameters*

The variations in $\Delta_{tt'}(T)$ as functions of the temperature for these nuclei are shown in Figs 4 to 6 for the approaches NP-1, NP-2, LP-1 and LP-2. Let us note that the values of NP-2 method are extracted from Ref. [101] where the temperature values only go up to 2 MeV. Let us also note that for the nuclei ^{36}Ar and ^{64}Ge, the "experimental" values of $\Delta_{tt'}(0)$ are less well reproduced in the case of model NP-2 than in that of model NP-1.

For the three considered nuclei, the $\Delta_{tt}(T)$ of the NP-1 and LP-1 methods overlap as it was the case in the schematic case. We have not found an explanation for this fact.

Moreover, the overall behavior of the three gap parameters of the present method is similar to that of the standard FTBCS method (LP-2). The abrupt increase in the Δ_{nn} and Δ_{pp} curves, and the abrupt decrease in the Δ_{np} one at $T = T_{cnp}$ that appear in NP-2 method no longer exist in NP-1 method.

Besides, the critical temperatures of the present model are clearly more important than the ones predicted by NP-2 and LP-2 methods. Their values are more than twice those predicted by NP-2 and LP-2 models.

2. *Excitation energy*

The variations in $E_{exc}(T)$ as functions of the temperature are reported in the same figure as $\Delta_{tt'}$ for each of the considered nuclei. We can than see a change in the slope of E_{exc} at the various critical temperatures. However, the change in the isovector pairing case is less sudden within the framework of NP-1 model than within the NP-2 one. This is a direct consequence of the behavior of $\Delta_{tt'}(T)$.

For all the considered nuclei, the excitation energy of NP-2 model increases faster than that of NP-1, until $T = T_{cnn}$ of NP-2 model. Beyond this value, the situation is inverted.

We have then have evaluated the isovector pairing effect on the excitation energy using the quantities δE_{exc1} and δE_{exc2} defined by Eqs (48) and (49). Their respective values at $T = (T_{cnp})_1$ and $T = (T_{cnp})_2$ are given in Table

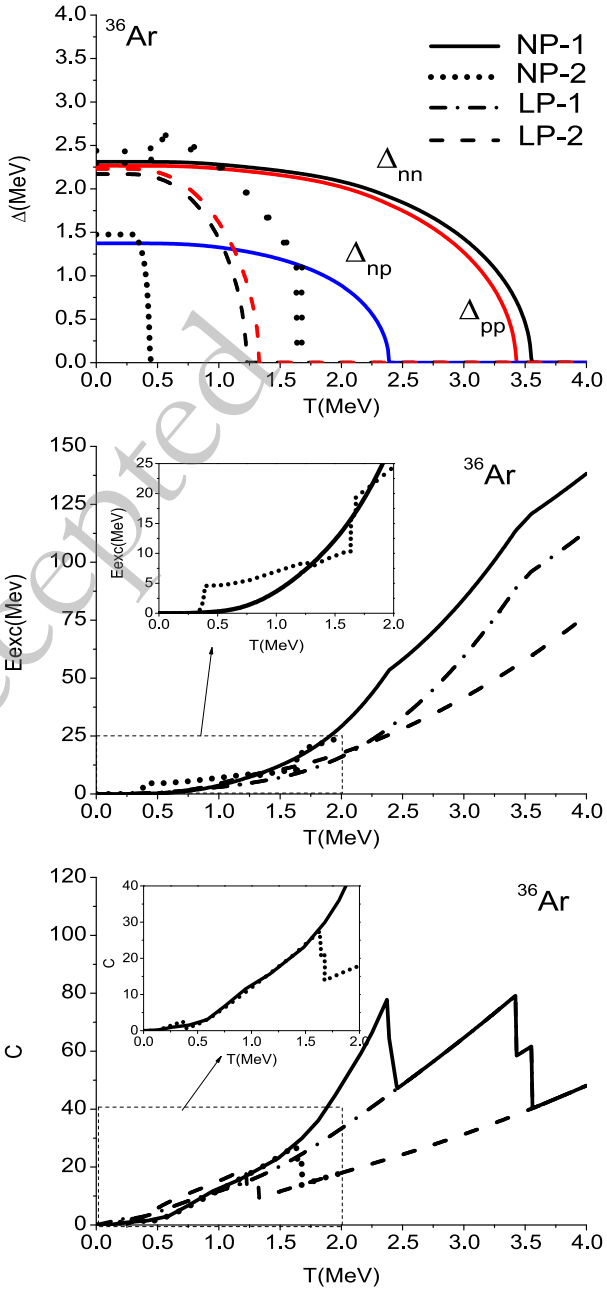

Fig. 4. (color online) Variation in the pairing gap parameters $\Delta_{tt'}(T)$, $t,t'=n,p$ (upper part), the excitation energy E_{exc} (middle), and heat capacity C as functions of the temperature T for the nucleus ^{36}Ar. Solid lines refer to the NP-1 model (present work), dotted lines refer to the NP-2 model (Refs [100−102]) in the isovector pairing case. Dash-dotted lines refer to the LP-1 model (Ref. [104]) and dashed lines refer to the LP-2 (standard FTBCS) model in the pairing between like-particles case. The Δ_{nn} and Δ_{pp} curves in NP-1 and LP-1 models are exactly superposed.

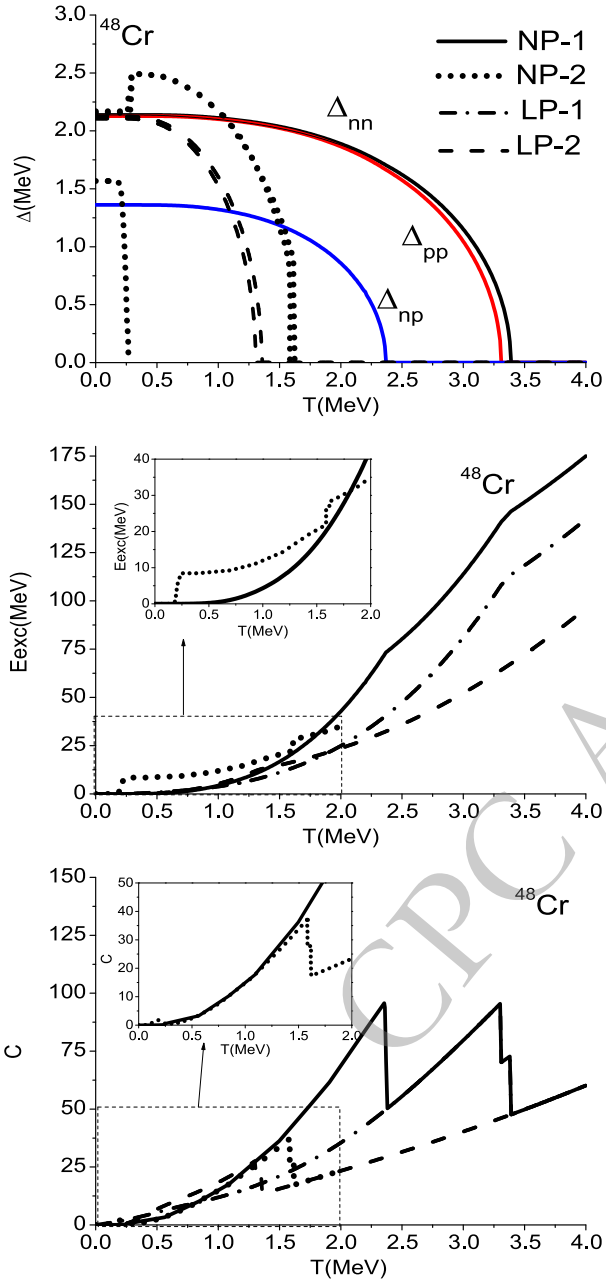

Fig. 5. (color online) Same as Fig. 4 for the nucleus ^{48}Cr

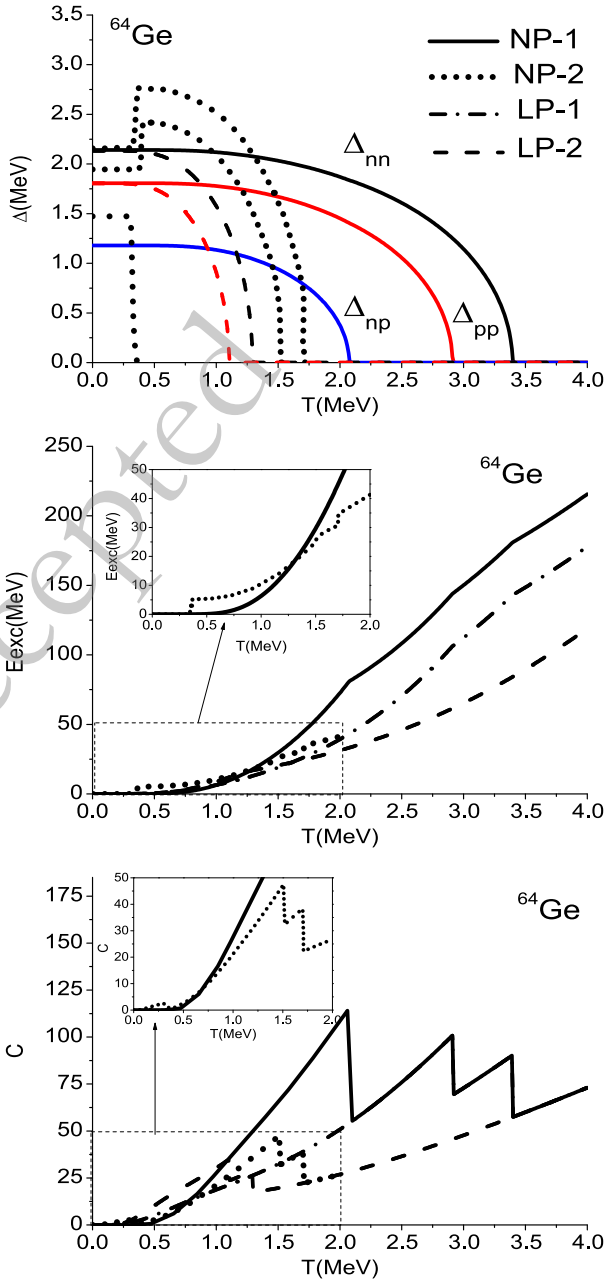

Fig. 6. (color online) Same as Fig. 4 for the nucleus ^{64}Ge

1. It then appears that the np pairing contribution to the excitation energy is much more important in the framework of the NP-1 model than in the NP-2 one.

When $T > T_{cnn}$ of NP-1 model, all curves are parallel since there is no more pairing in this region. Nevertheless, as in the schematic case, the excitation energy graphs are not superposed because the energy values at zero temperature are different in the various approaches.

3. *Heat capacity*

The variations in $C(T)$ as functions of the temperature are shown in Figs 4 to 6. As in the schematic case, the overall behavior is similar for the four approaches: none of them can reproduce the S-shaped curve of the experimental heat capacities.

Table 1. Isovector pairing effect on the excitation energy evaluated at the neutron-proton critical value of the temperature. (see the text for notations)

Nucleus	$\delta E_{exc1}\left(\left(T_{cnp}\right)_1\right)(MeV)$	$\delta E_{exc2}\left(\left(T_{cnp}\right)_2\right)(MeV)$
^{36}Ar	24.86	2.51
^{48}Cr	32.76	8.46
^{64}Ge	37.76	5.06

For nuclei ^{36}Ar and ^{48}Cr, the "experimental" values of $\Delta_{nn}(0)$ and $\Delta_{pp}(0)$ are very close to each other. The $\Delta_{tt}(T)$, $t=,np$, curves are then practically superposed in all the models. It follows that the peaks in $C(T)$ curves at T_{cnn} and T_{cpp} are very close and in some cases they are difficult to distinguish.

There exists a shift between the peaks positions at $T=T_{cnn}$ and $T=T_{cpp}$ between the NP-2 and LP-2 models. It is obviously due to the shift observed in the $\Delta_{tt}(T)$ graphs between these two models. This shift no more exist between the NP-1 and LP-1 approaches: the $C(T)$ curves are exactly superposed when $T>(T_{cnp})_1$.

In the isovector pairing case, the height of the peak in NP-2 approach at $T=(T_{cnp})_2$ is small compared to the peaks corresponding to the proton and neutron critical temperature values. However the peak in NP-1 approach at $T=(T_{cnp})_1$ is comparable to that of its homologues at $T=T_{cnn}$ and $T=T_{cpp}$. Moreover, the peak at $T=(T_{cnp})_2$ is negligible compared to the one at $T=(T_{cnp})_1$.

In the temperature range between $(T_{cnp})_2$ and T_{cpp} of NP-2 approach, the NP-1 and NP-2 curves are very close to each other for the nuclei ^{36}Ar and ^{48}Cr. The discrepancy observed in the ^{64}Ge case is probably due to the fact that the $\Delta_{tt'}(0)$, $t,t'=n,p$, values are different in the two models.

All the curves for the four considered models join when $T>T_{cnn}$ of model NP-1, since there is no more pairing in this region.

In summary, the main conclusions drawn in the schematic case remain valid in the realistic case.

However, the predicted critical temperatures seem to be too high. In the pairing between like-particles case, it was found in Ref. [104] that the LP-1 approach reproduces well the exact results of the gap parameter, the energy and the heat capacity at low temperature. But this is no longer the case at higher temperatures. This leads to an overestimation of the energy values for higher temperatures.

As the NP-1 approach is a generalization of LP-1, it can be assumed that the $\Delta_{tt'}$, $_{t,t'=n,p}$, E_{exc} and C are correctly described by the NP-1 approach at low temperature. However, Tthe latter seems to overestimate the critical temperatures, which leads to excessive values of E_{exc}. To remedy this problem, the thermal and quantal fluctuations should be taken into account and a particle-number projection should be performed.

VI. CONCLUSION

We present a model for the treatment of the temperature dependent np pairing correlations based on the path integral formalism (model NP-1). It generalizes the recently proposed model using a similar approach in the pairing between like-particles case (model LP-1).

The pairing terms in the total Hamiltonian are written in a square form in order to facilitate the use of the Hubbard-Stratonovitch transformation. The expression for the partition function of the system is then established using the static path approximation.

The gap equations, as well as the expressions for the energy, the entropy and the heat capacity of the system are deduced. They do generalize those of LP-1 model. Indeed, one simply has to set $\Delta_{np}=0$ in the expressions of NP-1 model to find the equations of the LP-1 model. Moreover, they are different from the ones obtained within the NP-2 model (which a generalization of the standard FTBCS model LP-2) because the approximations used are of a different nature.

As a first step, the formalism is numerically applied within the framework of the schematic Richardson model. The method is in a second step applied to realistic cases using the single-particle energies of a deformed Woods-Saxon mean-field. Three nuclei such as $N=Z$ are considered since the np pairing is supposed to be maximal in this kind of systems: ^{36}Ar, ^{48}Cr and ^{64}Ge.

The variations in the three gap parameters, the excitation energy and the heat capacity are studied as functions of the temperature in both schematic and realistic cases. They are compared to the results of the LP-1, NP-2 and LP-2 approaches. The conclusions in the schematic and realistic cases are similar.

It is shown that the behavior of the three gap parameters of NP-1 model is similar to that of $\Delta_{tt}(T)$ in the standard FTBCS model. One notes the existence of critical values of the temperature beyond which $\Delta_{tt'}$, $t,t'=n,p$, vanish. These critical temperatures are significantly larger in models NP-1 and LP-1 than in models NP-2 and LP-2. Moreover, the $\Delta_{tt}(T)$, of the NP-1 and LP-1 models are exactly superposed, while those of the NP-2 and LP-2 models are different. Furthermore, the sudden variation in the graphs of $\Delta_{tt}(T)$ in the vicinity of T_{cnp} in the NP-2 model no longer exists in the NP-1 model.

Dealing with the excitation energy, it appears that the isovector np pairing contribution to this quantity predicted by NP-1 model is more important than the one predicted by NP-2 model.

Finally, the heat capacity exhibits an overall behavior which is similar in the four approaches: none of them can reproduce the S-shaped curve of the experimental heat capacities. In each model, there is a peak at each value of the critical temperature. These peaks are significantly higher in the framework of the models NP-1 and LP-1 than in the framework of the models NP-2 and LP-2.

Let us however note that there is no experimental data available for the considered nuclei, it is therefore difficult to decide between the different approaches. Nevertheless, the model NP-1 seems to overestimate the critical temperatures. To remedy this problem, the thermal and quantal fluctuations should be taken into account and a

particle-number projection should be performed.

It would also be interesting to generalize the present study to the isovector plus isoscalar pairing case.

APPENDIX A. CALCULATION DETAILS OF R_{np}^2

Let us consider the unitary operator

$$U_{np} = U_n U_p \tag{A1}$$

with

$$U_t = \prod_{j>0} \mathcal{S}_{jt}\ ,\ \mathcal{S}_{jt} = i\left(a_{jt} + a_{jt}^+\right)\left(a_{\tilde{j}t} + a_{\tilde{j}t}^+\right),\ t = n, p. \tag{A2}$$

We can easily verify that

$$U_{np}^+ = U_{np}. \tag{A3}$$

Operators $P_{np}^+ U_{np}$ and $U_{np}^+ P_{np}$ are identical and are given by

$$P_{np}^+ U_{np} = U_{np}^+ P_{np} = R_{np} \tag{A4}$$

where

$$R_{np} = \sum_{\nu>0}\left[\eta_{\nu n}\eta_{\tilde{\nu}p}B_{\nu n\tilde{p}} + \eta_{\nu p}\eta_{\tilde{\nu}n}B_{\nu p\tilde{n}}\right] \tag{A5}$$

with

$$B_{\nu n\tilde{p}} = \left(a_{\tilde{\nu}n} + a_{\tilde{\nu}n}^+\right)\left(a_{\nu p} + a_{\nu p}^+\right)\prod_{\substack{j>0\\ j\neq\nu}} \mathcal{S}_{jn}\,\mathcal{S}_{jp} \tag{A6}$$

$$B_{\nu p\tilde{n}} = \left(a_{\tilde{\nu}p} + a_{\tilde{\nu}p}^+\right)\left(a_{\nu n} + a_{\nu n}^+\right)\prod_{\substack{j>0\\ j\neq\nu}} \mathcal{S}_{jn}\,\mathcal{S}_{jp}. \tag{A7}$$

Finally, we have

$$P_{np}^+ P_{np} = P_{np}^+ U_{np} U_{np}^+ P_{np} = R_{np}^2. \tag{A8}$$

APPENDIX B. CALCULATION DETAILS OF Z

Let us set in Eq. (8)

$$\begin{aligned}\mathsf{S}_{tt'}(\beta) &= T_\tau\ \exp\left(\int_0^\beta H_{tt'}(\tau)d\tau\right)\\ &= \lim_{N\to\infty} T_\tau \prod_{i=1}^{N}\exp\left(\frac{\beta}{N}H_{tt'}(\tau_i)\right)\ ,\ t,t' = n,p.\end{aligned} \tag{B1}$$

We then have

$$\mathsf{S}(\beta) = \mathsf{S}_{nn}(\beta)\,\mathsf{S}_{pp}(\beta)\,\mathsf{S}_{np}(\beta). \tag{B2}$$

Using the Hubbard-Stratonovitch transformation [91], [105, 106]

$$\exp\left(O^2\right) = \int_{-\infty}^{+\infty} dx \exp\left\{-\pi x^2 - 2\sqrt{\pi}xO\right\}, \tag{B3}$$

where O is a bounded Hermitian operator and x is an external field, the quantities $\mathsf{S}_{tt'}(\beta)$, become

$$\begin{aligned}\mathsf{S}_{tt'}(\beta) = T_\tau \lim_{N\to\infty}\prod_{i=1}^{N}\int_{-\infty}^{+\infty}\sqrt{\frac{\beta}{N}}dX_{tt'i}\exp\left\{-\pi\frac{\beta}{N}X_{tt'i}^2\right.\\ \left.-2\frac{\beta}{N}\sqrt{\pi G_{tt'}}X_{tt'i}R_{tt'}(\tau_i)\right\}\end{aligned} \tag{B4}$$

where we set, for simplicity

$$x_{tt'i} = x_{tt'}(\tau_i), \tag{B5}$$

and $X_{tt'i}$ is such that

$$x_{tt'i} = \sqrt{\frac{\beta}{N}}X_{tt'i}. \tag{B6}$$

At the limit where N goes to infinity, we set

$$\int \mathfrak{D}X_{tt'} = \lim_{N\to\infty}\int_{-\infty}^{+\infty}\prod_{j=1}^{N}\sqrt{\frac{\beta}{N}}dX_{tt'j}. \tag{B7}$$

It is worth noticing that $X_{tt'j}$ means here $X_{tt'}(\tau_j)$ and that when the limit is taken, $X_{tt'j} \to X_{tt'}(\tau)$.

$\mathsf{S}_{tt'}(\beta)$ finally reads

$$\begin{aligned}S_{tt'}(\beta) = T_\tau\int\mathfrak{D}X_{tt'}\exp\left\{-\pi\int_0^\beta X_{tt'}^2(\tau)d\tau\right.\\ \left.-2\sqrt{\pi G_{tt'}}\int_0^\beta R_{tt'}(\tau)X_{tt'}(\tau)d\tau\right\}.\end{aligned} \tag{B8}$$

Let us set

$$\Delta_{tt'}(\tau) = \sqrt{\pi G_{tt'}}X_{tt'}(\tau), \tag{B9}$$

the partition function Z is then given by

$$Z = T_\tau Tr \int \mathfrak{D}\Delta_{nn}\mathfrak{D}\Delta_{pp}\mathfrak{D}\Delta_{np} \times \exp\left\{-\int_0^\beta \left[\frac{\Delta_{nn}^2(\tau)}{G_{nn}} + \frac{\Delta_{pp}^2(\tau)}{G_{pp}} + \frac{\Delta_{np}^2(\tau)}{G_{np}}\right] d\tau\right\} \times \exp\left\{-\beta H_0 - 2\int_0^\beta \left[R_{nn}(\tau)\Delta_{nn}(\tau) + R_{pp}(\tau)\Delta_{pp}(\tau) + R_{np}(\tau)\Delta_{np}(\tau)\right] d\tau\right\}, \tag{B10}$$

where

$$\int \mathfrak{D}\Delta_{tt'} = \lim_{N\to\infty} \int_{-\infty}^{+\infty} \prod_{j=1}^{N} \sqrt{\frac{\beta}{N}} \frac{1}{\sqrt{\pi G_{tt'}}} d\Delta_{tt'j}. \tag{B11}$$

Using the static-path approximation [107], where it is assumed that $\Delta_{tt'}(\tau)$ is independent of τ, i.e.:

$$\Delta_{tt'}(\tau) = \Delta_{tt'}, \tag{B12}$$

Z reduces to ordinary integrals over the variables $\Delta_{tt'}$. It then reads as

$$Z = \frac{1}{\pi^{3/2}\sqrt{G_{nn}G_{pp}G_{np}}} \int d\Delta_{nn} d\Delta_{pp} d\Delta_{np} \times \exp\left\{-\beta\left[\frac{|\Delta_{nn}|^2}{G_{nn}} + \frac{|\Delta_{pp}|^2}{G_{pp}} + \frac{|\Delta_{np}|^2}{G_{np}}\right]\right\} Tr \times \exp\left(-\beta\sum_\nu h_{\nu np}\right) \tag{B13}$$

with

$$h_{\nu np} = \tilde{\varepsilon}_{\nu n}(\eta_{\nu n} + \eta_{\tilde{\nu}n}) + \tilde{\varepsilon}_{\nu p}\left(\eta_{\nu p} + \eta_{\tilde{\nu}p}\right) + 2\Delta_{nn}\eta_{\nu n}\eta_{\tilde{\nu}n}B_{\nu n} + 2\Delta_{pp}\eta_{\nu p}\eta_{\tilde{\nu}p}B_{\nu p} + 2\Delta_{np}\left(\eta_{\nu n}\eta_{\tilde{\nu}p}B_{\nu n\tilde{p}} + \eta_{\tilde{\nu}n}\eta_{\nu p}B_{\nu p\tilde{n}}\right) \tag{B14}$$

APPENDIX C. COMMUTATOR $\left[h_{\nu pn}, h_{\mu np}\right]$

Let us set

$$h_{\nu np} = \sum_t h_{\nu t} + h'_{\nu np} \tag{C1}$$

with

$$h_{\nu t} = \tilde{\varepsilon}_{\nu t}(\eta_{\nu t} + \eta_{\tilde{\nu}t}) + 2\Delta_{tt}\eta_{\nu t}\eta_{\tilde{\nu}t}B_{\nu t} \tag{C2}$$

and

$$h'_{\nu np} = 2\Delta_{np}\left(\eta_{\nu n}\eta_{\tilde{\nu}p}B_{\nu n\tilde{p}} + \eta_{\tilde{\nu}n}\eta_{\nu p}B_{\nu p\tilde{n}}\right). \tag{C3}$$

The commutation relation between $h_{\nu np}$ and $h_{\mu np}$ is given by

$$\left[h_{\nu np}, h_{\mu np}\right] = \sum_{tt'}\left[h_{\nu t}, h_{\mu t'}\right] + \sum_t\left[h_{\nu t}, h'_{\mu np}\right] + \sum_t\left[h'_{\nu np}, h_{\mu t}\right] + \left[h'_{\nu np}, h'_{\mu np}\right]. \tag{C4}$$

We then have

$$\left[h_{\nu t}, h_{\mu t'}\right] = 2\Delta_{t't'}\tilde{\varepsilon}_{\nu t}\left[(\eta_{\nu t} + \eta_{\tilde{\nu}t}), \eta_{\mu t'}\eta_{\tilde{\mu}t'}B_{\mu t'}\right] + 2\Delta_{tt}\tilde{\varepsilon}_{\mu t'}\left[\eta_{\nu t}\eta_{\tilde{\nu}t}B_{\nu t}, (\eta_{\mu t'} + \eta_{\tilde{\mu}t'})\right] + 4\Delta_{tt}\Delta_{t't'}\left[\eta_{\nu t}\eta_{\tilde{\nu}t}B_{\nu t}, \eta_{\mu t'}\eta_{\tilde{\mu}t'}B_{\mu t'}\right]. \tag{C5}$$

The first two terms in $\left[h_{\nu t}, h_{\mu t'}\right]$ for $\nu \neq \mu$, are proportional to $\Delta_{t't'}$ (and thus to $\sqrt{G_{t't'}}$) or to Δ_{tt} (and thus to $\sqrt{G_{tt}}$). As for the last one, it is proportional to the product $\Delta_{tt}\Delta_{t't'}$ (and thus to $\sqrt{G_{tt}G_{t't'}}$).

In the same way, $\left[h_{\nu t}, h'_{\mu np}\right]$ and $\left[h'_{\nu np}, h_{\mu t}\right]$ for $\nu \neq \mu$, are the sum of a term proportional to Δ_{np} (and thus to $\sqrt{G_{np}}$) and another one proportional to $\Delta_{tt}\Delta_{np}$ (and thus to $\sqrt{G_{tt}G_{np}}$). For example,

$$\left[h_{\nu t}, h'_{\mu np}\right] = 2\Delta_{np} \times \left[\tilde{\varepsilon}_{\nu t}(\eta_{\nu t} + \eta_{\tilde{\nu}t}), \left(\eta_{\mu n}\eta_{\tilde{\mu}p}B_{\mu n\tilde{p}} + \eta_{\tilde{\mu}n}\eta_{\mu p}B_{\mu p\tilde{n}}\right)\right] + 4\Delta_{tt}\Delta_{np}\left[(\eta_{\nu t}\eta_{\tilde{\nu}t}B_{\nu t}), \left(\eta_{\mu n}\eta_{\tilde{\mu}p}B_{\mu n\tilde{p}} + \eta_{\tilde{\mu}n}\eta_{\mu p}B_{\mu p\tilde{n}}\right)\right]. \tag{C6}$$

Finally, $\left[h'_{\nu np}, h'_{\mu np}\right]$ for $\nu \neq \mu$, is proportional to Δ_{np}^2 (and thus to G_{np}). As the values of $G_{tt'}$ $(t, t' = n, p)$ are small compared to single-particle energies, the approximation

$$\left[h_{\nu np}, h_{\mu np}\right] = 0\ ,\ \nu \neq \mu,$$

is justified.

APPENDIX D. ISOVECTOR PAIRING GAP EQUATIONS (NP-2 MODEL REF. [100])

The temperature dependent gap equations in the isovector pairing case of Ref. [100] are briefly recalled in the

following.

The gap parameters $\Delta_{tt'}$ $(t,t'=n,p)$ are defined by

$$\frac{4\Delta_{nn}}{G_{nn}} = \sum_{\nu,\,\tau=1,2}\frac{1}{E_{\nu\tau}}\tanh\frac{1}{2}\beta E_{\nu\tau}\left\{\Delta_{nn}+\frac{(-1)^{\tau+1}}{R_\nu}\times\left[\left(E_{\nu n}^2-E_{\nu p}^2\right)\Delta_{nn}+2\Delta_{np}^2\left(\Delta_{nn}+\Delta_{pp}\right)\right]\right\} \tag{D1}$$

$$\frac{4\Delta_{pp}}{G_{pp}} = \sum_{\nu,\,\tau=1,2}\frac{1}{E_{\nu\tau}}\tanh\frac{1}{2}\beta E_{\nu\tau}\left\{\Delta_{pp}+\frac{(-1)^{\tau+1}}{R_\nu}\left[\left(E_{\nu p}^2-E_{\nu n}^2\right)\Delta_{pp}+2\Delta_{np}^2\left(\Delta_{nn}+\Delta_{pp}\right)\right]\right\} \tag{D2}$$

$$\frac{2}{G_{np}} = \sum_{\nu,\,\tau=1,2}\frac{1}{E_{\nu\tau}}\tanh\frac{1}{2}\beta E_{\nu\tau}\times\left\{1+\frac{(-1)^{\tau+1}}{R_\nu}\left[E_{\nu n}^2+E_{\nu p}^2+2\left(\Delta_{nn}\Delta_{pp}-\tilde{\varepsilon}_{\nu n}\tilde{\varepsilon}_{\nu p}\right)\right]\right\}. \tag{D3}$$

with the notations

$$E_{\nu\tau}^2 = \frac{1}{2}\left\{E_{\nu n}^2+E_{\nu p}^2+2\Delta_{np}^2+(-1)^{\tau+1}R_\nu\right\},\ \tau=1,2 \tag{D4}$$

$$R_\nu^2 = \left(E_{\nu n}^2-E_{\nu p}^2\right)^2+4\Delta_{np}^2\left[\left(\tilde{\varepsilon}_{\nu n}-\tilde{\varepsilon}_{\nu p}\right)^2+\left(\Delta_{nn}+\Delta_{pp}\right)^2\right] \tag{D5}$$

and

$$E_{\nu t} = \sqrt{\tilde{\varepsilon}_{\nu t}^2+\Delta_{tt}^2}. \tag{D6}$$

The particle-number conservation conditions are given by

$$N_t = \sum_\nu\left\{1+\sum_{\tau=1,2}\frac{\partial E_{\nu\tau}}{\partial\lambda_t}\tanh\frac{1}{2}\beta E_{\nu\tau}\right\} \tag{D7}$$

with

$$\frac{\partial E_{\nu\tau}}{\partial\lambda_{n(p)}} = \frac{1}{2E_{\nu\tau}}\left\{-\tilde{\varepsilon}_{\nu n(p)}+(-1)^{\tau+1}\frac{1}{R_\nu}\times\left[\tilde{\varepsilon}_{\nu n(p)}\left(E_{\nu p(n)}^2-E_{\nu n(p)}^2\right)+2\Delta_{np}^2\left(\tilde{\varepsilon}_{\nu p(n)}-\tilde{\varepsilon}_{\nu n(p)}\right)\right]\right\}. \tag{D8}$$

At the limit when $\Delta_{np}=0$, Eqs. (D1) and (D2) become

$$\frac{2}{G_{tt}} = \sum_\nu\frac{1}{E_{\nu t}}\tanh\left(\frac{\beta}{2}E_{\nu t}\right) \tag{D9}$$

and the particle-number conservation conditions (87) become

$$N_t = \sum_\nu\left[1-\frac{\tilde{\varepsilon}_{\nu t}}{E_{\nu t}}\tanh\left(\frac{\beta}{2}E_{\nu t}\right)\right]. \tag{D10}$$

The latter equations are the standard FTBCS expressions [45], [47], [101], [103].

References

[1] J. Bardeen, L. N. Cooper and J. R. Schrieffer, Phys. Rev. **108**(5), 1175 (1957)
[2] S.T. Belyaev, Mat. Fys. Medd. Dan. Vid. Selsk. **31**, 11 (1959)
[3] A. Goswami, Nucl. Phys. **60**(2), 228 (1964)
[4] A. Goswami and L.S. Kisslinger, Phys. Rev. **140**(1B), B26 (1965)
[5] H. T. Chen and A. Goswami, Nucl. Phys. **88**, 208 (1966)
[6] H. Chen and A. Goswami, Phys. Lett. B **24**, 257 (1967)
[7] M. Assié, H. Jacob, Y. Blumenfeld, V. Girard-Alcindor, arXiv: 2410.14314.
[8] A. L. Goodman, Nucl. Phys. A **186**, 475 (1972)
[9] A. L. Goodman, Adv. Nucl. Phys. **11**, 263 (1979)
[10] J. Engel, S. Pittel, M. Stoitsov, *et al.*, Phys. Rev. C **55**, 1781 (1997)
[11] O. Civitarese and M. Reboiro, Phys. Rev. C **56**, 1179 (1997)
[12] F. Simkovic, Ch. C. Moustakidis, L. Pacearescu and A. Faessler, Phys. Rev. C; **68**, 054319 (2003)
[13] D. Mokhtari, N. H. Allal and M. Fellah, Acta Phys. Hung. A: Heavy Ion Phys. **19**, 187 (2004)
[14] D. Mokhtari, M. Fellah and N. H. Allal, Int. J. Mod. Phys. E **25**, 1650035 (2016)
[15] S. Frauendorf and A.O. Macchiavelli, Progr. Part. Nucl. Phys. **78**, 24 (2014)
[16] C. Qi and R. Wyss, Phys. Scr. **91**, 013009 (2016)
[17] D. Mokhtari, I. Ami, M. Fellah, and N.H. Allal, Int. J. Mod. Phys. E **17**, 655 (2008)
[18] F. Hammache, N.H. Allal and M. Fellah, Int. J. Mod. Phys. E **21**, 1250100 (2012)
[19] H. J. Lipkin, Ann. Phys. (NY) **12**, 452 (1960)
[20] Y. Nogami, Phys. Rev. **134**, B313 (1964)
[21] W. Satula and R. Wyss, Phys. Lett. B **393**, 1 (1997)
[22] W. Satula and R. Wyss, Nucl. Phys. A **676**, 120 (2000)
[23] K. Sieja and A. Baran, Acta Phys. Pol. B **35**, 107 (2006)
[24] M. V. Stoitsov, J. Dobaczewski, R. Kirchner, *et al.*, Phys. Rev. C **76**, 014308 (2007)
[25] H. Olofsson, R. Bengtsson and P. Moller, Nucl. Phys. A

784, 104 (2007)
[26] A. A. Raduta, M. I. Krivoruchenko and Amand Faessler, Phys. Rev. C **85**, 054314 (2012)
[27] N. H. Allal, M. Fellah, M. R. Oudih, *et al*., Eur. Phys. J. A **27**(s01), 301 (2006)
[28] N. Sandulescu, B. Erren and J. Dukelsky, Phys. Rev. C **80**, 044335 (2009)
[29] S. Kerrouchi, D. Mokhtari, N.H. Allal, *et al*., Int. J. Mod. Phys. E **18**, 141 (2009)
[30] A. Berbiche, M. Fellah and N.H. Allal, J. Theor. Appl. Phys. **8**, 118 (2014)
[31] M. Fellah, N. H. Allal, Faiza Hammache, *et al*., Int. J. Mod. Phys. E **24**, 1550097 (2015)
[32] M. Douici, N.H. Allal, M. Fellah, N. Benhamouda, *et al*., Int. J. Mod. Phys. E **22**, 1350029 (2013)
[33] S. Kerrouchi, N.H. Allal, M. Fellah, *et al*., Int. J. Mod. Phys. E **19**, 1383 (2010)
[34] S. Kerrouchi, N. H. Allal, M. Fellah, *et al*., Int. J. Mod. Phys. E **24**, 1550014 (2015)
[35] N. H. Allal, M. Fellah, M. Douici, *et al*., Int. J. Mod. Phys. E **25**, 1650108 (2016)
[36] Faiza Hammache, N.H. Allal, M. Fellah, *et al*., Int. J. Mod. Phys. E **25**, 1650032 (2016)
[37] Y. Benbouzid, N.H. Allal, M. Fellah, *et al*., Chinese Phys. C **42**, 044103 (2018)
[38] Y. Benbouzid, N.H. Allal, M. Fellah, *et al*., Chinese Phys. C **42**, 084104 (2018)
[39] K. Uzawa, N. Hinohara and T. Nakatsukasa, Prog. Theor. Exp. Phys. **2024**(5), 053D02 (2024)
[40] M. Sambataro and N. Sandulescu, Phys. Lett. B **820**, 136476 (2021)
[41] F. Pan, C. Qi, L. Dai, *et al*., Europhys. Lett. **132**, 32001 (2020)
[42] F. Pan, Y. He, L. Dai, *et al*., Symmetry **13**, 1405 (2021)
[43] Y. P. Wang, Y. K. Wang, F. F. Xu, *et al*., Phys. Rev. Lett. **132**, 232501 (2024)
[44] J. Zhang, D. Lacroix and Y. Beaujeault-Taudiere, Phys. Rev. C **110**, 064330 (2024)
[45] M. Sano and S. Yamazaki, Prog. Theor. Phys. **29**(3), 397 (1963)
[46] L. G. Moretto, Nucl. Phys. A **185**(1), 145 (1972)
[47] A.L. Goodman, Phys. Rev. C **29**(5), 1887 (1984)
[48] H. Nakada and K. Tanabe, Int. J. Mod. Phys. E **15**(8), 1761 (2006)
[49] Z. Kargar, Phys. Rev. C **75**, 064319 (2007)
[50] K. Esashika, H. Nakada and K. Tanabe, Phys. Rev. C **72**, 044303 (2005)
[51] N. H. Allal, M. Fellah, N. Benhamouda, *et al*., Phys. Rev. C **77**, 054310 (2008)
[52] D. Gambacurta and D. Lacroix, Phys. Rev. C **85**, 044321 (2012)
[53] D. Gambacurta, D. Lacroix and N. Sandulescu, Phys. Rev. C **88**, 034324 (2013)
[54] W. Zhang and Y. F. Niu, Phys. Rev. C **96**, 054308 (2017)
[55] Z. Kargar and Z. Dehghani, J. Phys. G: Nucl. Part. Phys. **40**(4), 045108 (2013)
[56] Z. Kargar and R.N. Gashtaseb, Int. J. Mod. Phys. E **27**, 1850096 (2018)
[57] Z. Kargar and Sh. Afrookhteh, Results in Physics **52**, 106899 (2023)
[58] A. Goodman, Nucl. Phys. A **352**(1), 30 (1981)
[59] K. Tanabe, K. Sugawara-Tanabe and H. J. Mang, Nucl. Phys. A **357**(1), 20 (1981)
[60] N. Sandulescu, Phys. Rev. C **70**, 025801 (2004)
[61] Y. F. Niu, Z. M. Niu, N. Paar, *et al*., Phys. Rev. C **88**, 034308 (2013)
[62] Lang Liu, Zhen-Hua Zhang and Peng-Wei Zhao, Phys. Rev. C **92**, 044304 (2015)
[63] P. Fanto, Y. Alhassid, and G. F. Bertsch, Phys. Rev. C **96**, 014305 (2017)
[64] E. Yüksel, F. Mercier, J.-P. Ebran, *et al*., Phys. Rev. C **106**, 054309 (2022)
[65] B. Suleymanli, K. Bozkurt, E. Khan, *et al*., Phys. Rev. C **110**, 014329 (2024)
[66] A. Ravlić, Y. F. Niu, T. Nikšić, N. Paar, *et al*., Phys. Rev. C **104**, 064302 (2021)
[67] O. Civitarese, G.G. Dussel and R.P.J. Perazzo, Nucl. Phys. A **404**(1), 15 (1983)
[68] A. Storozhenko, P. Schuck, J. Dukelsky, *et al*., Annals of Physics **307**(2), 308 (2003)
[69] N. Dinh Dang and N. Quang Hung, Phys. Rev. C **77**, 064315 (2008)
[70] P. Fanto and Y. Alhassid, Phys. Rev. C **103**, 064310 (2021)
[71] A. Kaur, E. Yuksel and N. Paar, Phys. Rev. C **109**, 024305 (2024)
[72] Wei Zhang and Yi-Fei Niu, Chin. Phys. C **41**, 094102 (2017)
[73] Tao Yan, Yanlong Lin and Lang Liu, Phys. Rev. C **104**, 024303 (2021)
[74] Wei Zhang, Jin-Ke Huang and Yi-Fei Niu, Int. J. Mod. Phys. E **32**, 2340008 (2023)
[75] Yuhang Gao, Yanlong Lin and Lang Liu, Int. J. Mod. Phys. E **32**, 2350050 (2023)
[76] Yumen Wang, Yuhang Gao and Lang Liu, Chin. Phys. C **48**, 124104 (2024)
[77] E. Litvinova and P. Schuck, Phys. Rev. C **104**, 044330 (2021)
[78] M. Drissi and A. Rios, Eur. Phys. J. A **58**, 90 (2022)
[79] Kh. Benam, Eur. Phys. J. A **60**, 252 (2024)
[80] D. J. Dean and M. Hjorth-Jensen, Rev. Mod. Phys. **75**(2), 607 (2003)
[81] K. Langanke, P. Vogel and D.-C. Zhen, Nucl. Phys. A **626**(3), 735 (1997)
[82] S. E. Koonin, D. J. Dean and K. Langanke, Phys. Rep. **278**(1), 1 (1997)
[83] Y. Alhassid, G. F. Bertsch, C. N. Gilbreth, *et al*., Phys. Rev. C **93**, 044320 (2016)
[84] G. Puddu, Phys. Rev. B **45**(17), 9882 (1992)
[85] G. Puddu, Phys. Rev. C **47**(3), 1067 (1993)
[86] M. Marinus, H. G. Miller, R. M. Quick, *et al*., Phys. Rev. C **48**(4), 1713 (1993)
[87] R. Rossignoli, N. Canosa and J.L. Egido, Nucl. Phys. A **605**(1), 1 (1996)
[88] N. Canosa and R. Rossignoli, Phys. Rev. C **56**(2), 791 (1997)
[89] N. Canosa, R. Rossignoli and P. Ring, Phys. Rev. C **59**(1), 185 (1999)
[90] K. Kaneko and A. Schiller, Phys. Rev. C **76**, 064306 (2007)
[91] G. Fletcher, Am. J. Phys. **58**, 50 (1990)
[92] G. Martinez-Pinedo, K. Langanke and P. Vogel, Nucl. Phys. A **651**(4), 379 (1999)
[93] K. Kaneko and M. Hasegawa, Phys. Rev. C **72**, 031302 (2005)
[94] J. A. Sheikh, R. Palit and S. Frauendorf, Phys. Rev. C **72**,

041301 (2005)
[95] J.A. Sheikh, P.A. Ganai, R.P. Singh, *et al*., Phys. Rev. C **77**, 014303 (2018)
[96] K. Langanke, D. J. Dean, P. B. Radha, *et al*., Nucl. Phys. A **602**(2), 244 (1996)
[97] K. Langanke, D. J. Dean, S. E. Koonin, *et al*., Nucl. Phys. A **613**(3), 253 (1997)
[98] E. Yuksel, N. Paar, G. Colo, *et al*., Phys. Rev. C **101**, 044305 (2020)
[99] K. D. Duan, H. B. Zhang, and X. L. Shang, Phys. Rev. C **111**, 014320 (2025)
[100] M. Fellah, N.H. Allal, M. Belabbas, *et al*., Phys. Rev. C **76**, 047306 (2007)
[101] M. Belabbas, M. Fellah, N.H. Allal, *et al*., Int. J. Mod. Phys. E **19**(10), 1973 (2010)
[102] I. Ami, M. Fellah, N.H. Allal, *et al*., Int. J. Mod. Phys. E **20**(9), 1947 (2011)
[103] D. Mokhtari, N.H. Allal and M. Fellah, Int. J. Mod. Phys. E **27**, 1850054 (2018)
[104] M. Fellah, N.H. Allal and M. R. Oudih, Chin. Phys. C **48**(11), 114102 (2024)
[105] J. Hubbard, Phys. Rev. Lett. **3**(2), 77 (1959)
[106] R. L. Stratonovich, Sov. Phys. Dokl. **2**, 416 (1958)
[107] Y. Alhassid and J. Zingman, Phys. Rev. C **30**(2), 684 (1984)
[108] P. Ring and P. Schuck, *The Nuclear Many Body Problem* (Springer, Berlin, 1980).
[109] R. W. Richardson, and N. Sherman, Nucl. Phys. **52**, 253 (1964)
[110] T. Sumaryada and A. Volya, Phys. Rev. C **76**, 024319 (2007)
[111] E. Melby, *et al*., Phys. Rev. Lett. **83**(16), 3150 (1999)
[112] A. Schiller, A. Bjerve, M. Guttormsen, *et al*., Phys. Rev. C **63**, 021306 (2001)
[113] M. Guttormsen, R. Chankova, M. Hjorth-Jensen, *et al*., Phys. Rev. C **68**, 034311 (2003)
[114] N. H. Allal and M. Fellah, Phys. Rev. C **50**(3), 1404 (1994)